Co-Evaporated Bulk Heterojunction Solar Cells with > 6.0% Efficiency

ARTICLE *in* ADVANCED MATERIALS · MAY 2012

Impact Factor: 17.49 · DOI: 10.1002/adma.201200234 · Source: PubMed

7 AUTHORS, INCLUDING:

Hisahiro Sasabe
Yamagata University
93 PUBLICATIONS **2,970** CITATIONS
SEE PROFILE

Xiao-Feng Wang
Jilin University
44 PUBLICATIONS **828** CITATIONS
SEE PROFILE

Ziruo Hong
University of California, Los Angeles
129 PUBLICATIONS **7,134** CITATIONS
SEE PROFILE

ADVANCED MATERIALS
www.advmat.de

www.MaterialsViews.com

Co-Evaporated Bulk Heterojunction Solar Cells with >6.0% Efficiency

Guo Chen, Hisahiro Sasabe, Zhongqiang Wang, Xiao-Feng Wang, Ziruo Hong,* Yang Yang,* and Junji Kido*

The physical properties of organic compounds such as bandgaps, energy levels, and charge transport properties can be finely tuned via molecular design, which make them attractive for widespread applications in optoelectronics. There has been tremendous progresses in organic electronics during the past two decades; and much clear understanding on molecular design with respect to electronic properties in functional devices has been achieved.[1,2] Among the organic devices, organic photovoltaics (OPV) have attracted increasing attention due to its relatively simple processing requirements and the potential for fabricating light-weight large-area flexible solar panels.[3]

The bulk heterojunction between donor and acceptor molecules and their morphology control are the two critical criteria in realizing efficient photon-to-electron conversion. Recently, power conversion efficiency (PCE) of polymers and fullerene derivatives based photovoltaic cells has been reported exceeding 8% from several different polymer systems, and from tandem solar cell structures.[4,5] On one hand, it is very encouraging progress, since the efficiency has been increased dramatically within the past three years together with significant progress in fundamental understanding of the photophysics,[6] device physics,[7] and interface engineering.[8] It has been revealed in high performance OPV cells that percolation pathways for positive and negative charge transport can be formed via proper ways of morphology control and thin-film processing.[9–11] On the other hand, the difficult aspect of achieving even higher efficiency in polymer systems is the lack of precise control of the polydispersity index, regio-regularity, molecular weight, etc. These parameters have to be taken into account in thin-film processing, and have a strong correlation to the final photovoltaic performance.

An alternative materials strategy to polymers is to synthesize more monodisperse low molecular weight materials[12] or oligomers.[13,14] In addition to simple molecular structure, small molecule materials can be purified using traditional methods, for example re-crystallization and gel permeation chromatography from solutions for soluble materials, and vacuum sublimation from solid states if the materials can be thermally evaporated. Especially the latter offers high purity,[15,16] and has been shown to be effective to promote performance of organic optoelectronic devices.[17]

For small molecule materials, phthalocyanines (Pc) and their metal complexes are widely used due to their strong absorption and small bandgap.[18,19] However the drawback of Pc compounds is relatively low open circuit voltage (V_{oc}), which is determined by the offset between highest occupied molecular orbital (HOMO) of Pc compounds and lowest unoccupied molecular orbital (LUMO) of fullerene acceptors. That means the potential energy loss from photon to electron limits the overall PCE.

Among the small molecule materials, squaraine (SQ) dyes have shown tremendous potential for OPV cells due to their high absorption coefficients and intense absorption in the red and near-infrared (NIR) spectral regions.[20–23] Especially a squaraine dye 2,4-bis[4-(N,N-diisobutylamino)-2,6-dihydroxyphenyl] squaraine (DIB-SQ), as shown in **Figure 1**a, has bandgap of 1.7 eV, and HOMO level of 5.3 eV. Combining with fullerene C_{60} having LUMO level of ~4.0 eV, V_{oc} of DIB-SQ/C_{60} heterojunction is ~0.80 V.[24] As photoactive materials in thin film photovoltaic cells, the absorption coefficient has to be high enough to collect incident light within short optical path. To meet these requirements, SQ compounds have been regarded as one group of promising candidates. For example, strong absorption can be obtained even when the donor film is as thin as 65 Å. Based on such a layer, 3.0% PCE has been reported from thermally deposited photovoltaic cells.[24] On the other hand, it is yet necessary

G. Chen, Dr. H. Sasabe, Z. Q. Wang, Dr. X. F. Wang, Dr. Z. R. Hong, Prof. J. Kido
Department of Organic Device Engineering
Graduate School of Engineering,
and the Research Center for Organic Electronics (ROEL)
Yamagata University
4-3-16 Jonan, Yonezawa, Yamagata 992-8510, Japan
E-mail: h-sasabe@yz.yamagata-u.ac.jp; ziruo@yz.yamagata-u.ac.jp
Prof. Y. Yang
Department of Materials Science and Engineering
University of California-Los Angeles
Los Angeles, CA 90095, USA
E-mail: yangy@ucla.edu

DOI: 10.1002/adma.201200234

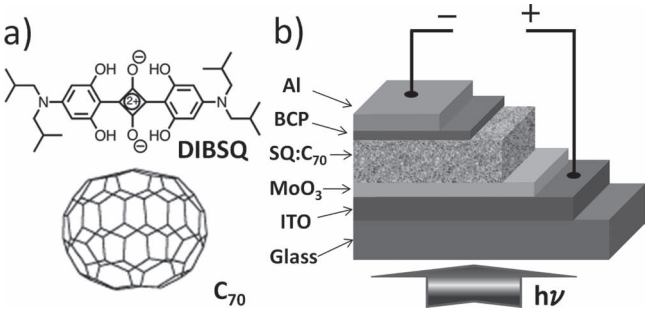

Figure 1. a) Molecular structures of a squaraine compound DIB-SQ and fullerene C_{70}; b) device architecture of the DIB-SQ:C_{70} photovoltaic cells.

to increase light harvesting, since it is obvious that the external quantum efficiency (EQE) corresponding to the photoresponse of SQ is below 30%. Improved efficiencies from bulk heterojunctions structures have also been reported by tuning the morphology of solution processed films.[10,25] Meanwhile, vacuum deposition is also useful to form high quality films without using solvents. A bulk heterojunction can be easily realized by co-deposition of two or more sources. Therefore, in this work, we fabricated bulk heterojunction photovoltaic cells based on DIB-SQ as a donor and fullerene C_{70} as an acceptor, and their chemical structures are shown in Figure 1a. The combination of such a donor/acceptor pair fully covers the spectral response from 320 nm to 700 nm. A high J_{sc} of 13.7 mA/cm^2 and PCE of 6.3% are obtained. Such efficiency represents one of the highest values reported on vacuum-deposited single heterojunctions.[26] Our data also indicates that the efficiency does not have strong dependence on the donor:acceptor ratio and thickness of blend films, which is important from a production point of view.

As shown in Figure 1b, the donor and acceptor are co-evaporated to form the blend films. In such a case, short exciton diffusion length of DIB-SQ is no longer a bottleneck for charge generation, and EQE from absorption of DIB-SQ reaches over 50%. MoO_3 as an anode buffer layer is thermally deposited on ITO surface to collect holes due to its deep conduction band.[27,28] Aluminum is used as a cathode with bathocuproine (BCP) as a buffer for efficient electron extraction.[29]

Our study is focused on the photovoltaic performance of DIB-SQ:C_{70} blend film, therefore no neat thin film is used, although the p-i-n type structure have proved effective for improving PCE.[17] We firstly investigated the effects of blending ratios on photovoltaic performance. **Table 1** contains the summary from various blending ratios of DIB-SQ:C_{70}. Note that integration of EQE data over standard AM1.5G spectrum yields calculated J_{sc} within 5% discrepancy comparing to measured J_{sc} under 100mW/cm^2 AM1.5G simulated solar light. 1:1 ratio yields PCE below 2.8%, the large serial resistance could be due to poor charge transports indicated in **Figure 2**a. As shown in Figure 2c, the EQE spectra consist of three major peaks at 360 nm, 520 nm and 700 nm approximately. The first two peaks located at 360 nm and 520 nm respectively, correspond to absorption of C_{70}, and the third peak at 700 nm is from DIB-SQ. With decreasing the blending ratio of DIB-SQ in blend films, the absorption peak of DIB-SQ blue-shift slightly as indicated in **Figure 3**, consistent with EQE and absorption data. This is due to chemical environment and aggregation states of DIB-SQ molecules.

From 1:1 ratio solar cells, the EQE at ~700 nm approaches 50%, which is significantly higher than previous study on planar heterojunction photovoltaic cells.[24] However the average EQE is still between 30% and 40% in visible range. As summarized

Table 1. Summary of the key parameters in 60 nm-thick DIB-SQ:C_{70} cells with various blend ratios.

Blend ratio	J_{sc} [mA/cm^2]	V_{oc} [V]	FF	PCE (%) [P_0 = 1 sun]
1:1	8.3 ± 0.1	0.77 ± 0.01	0.41 ± 0.01	2.7 ± 0.1
1:3	12.7 ± 0.1	0.81 ± 0.01	0.46 ± 0.01	4.7 ± 0.2
1:5	13.6 ± 0.1	0.86 ± 0.01	0.52 ± 0.01	6.1 ± 0.2
1:7.5	12.1 ± 0.1	0.90 ± 0.01	0.54 ± 0.01	5.9 ± 0.2
1:10	11.8 ± 0.1	0.93 ± 0.01	0.53 ± 0.01	5.8 ± 0.2
1:15	11.2 ± 0.1	0.94 ± 0.01	0.56 ± 0.01	5.9 ± 0.2
1:20	10.4 ± 0.1	0.94 ± 0.01	0.55 ± 0.01	5.4 ± 0.2

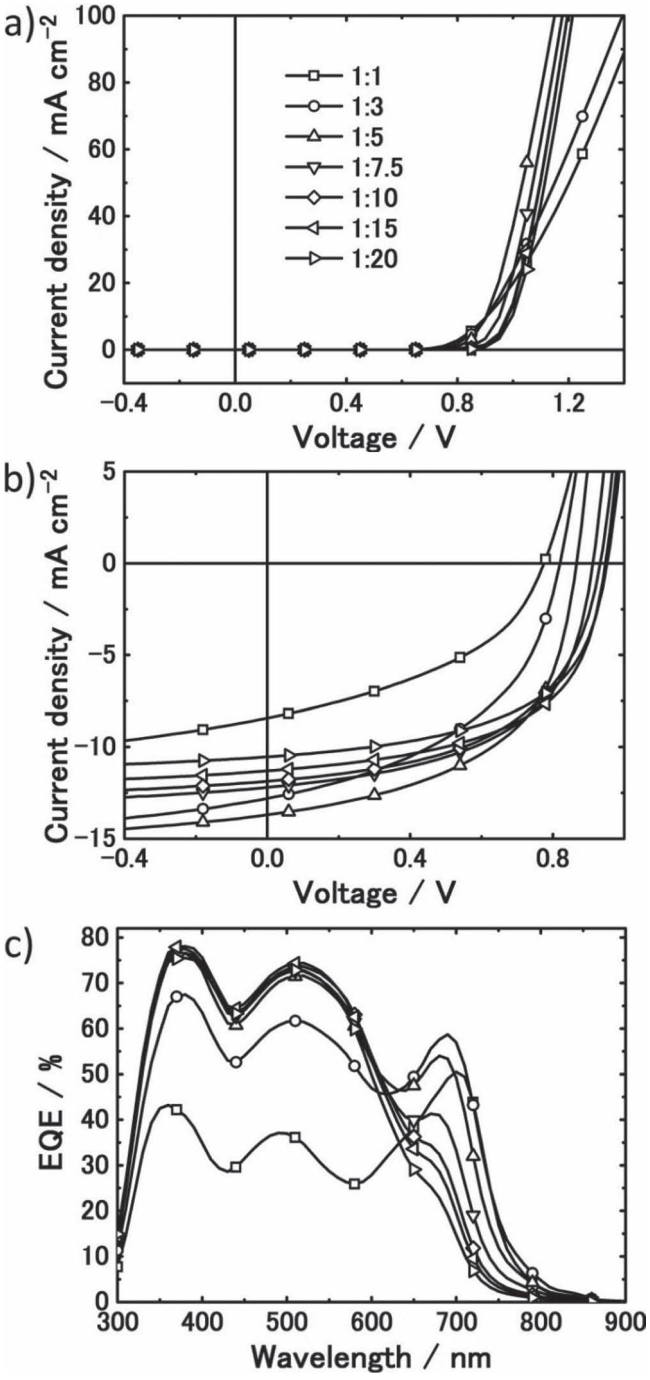

Figure 2. a) Dark J–V characteristics, b) J–V characteristics illuminated at 100 mW/cm^2 (AM 1.5G solar spectrum), c) EQE curves of solar cells based on 60nm-thick DIB-SQ:C_{70} blend film with various blend ratio.

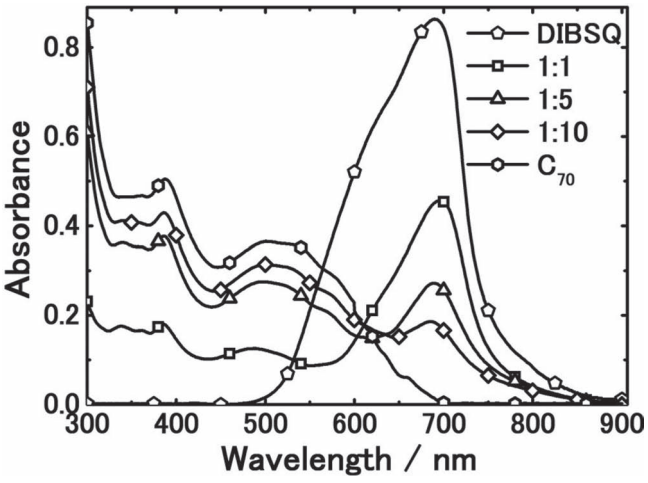

Figure 3. Absorbance of 60-nm-thick DIB-SQ film, C_{70} film and DIB-SQ:C_{70} blend films with blend ratio of 1:1, 1:5 and 1:10.

in Table 1, the device shows V_{oc} of 0.78 V, J_{sc} of 8.4 mA/cm^2, and FF of 42%. None of these parameters are satisfactory, and the low FF is due to both high serial resistance and strong bias dependent charge recombination.

Decreasing DIB-SQ loading in the blend film, 1:3 ratio of DIB-SQ:C_{70} slightly reduces the serial resistance. Though the recombination is still quite strong according to the slope of J–V curve at 0 V, PCE increases dramatically to 4.9%. V_{oc} and FF are improved slightly to 0.82 V and 47%, respectively. The J_{sc} increases dramatically, reaching 12.80 mA/cm^2. From the EQE in Figure 2c, the three peaks at 380 nm, 510 nm and 690 nm increase significantly. In comparison to 1:1 case, the peak at 690 nm is slightly enhanced, while the major increase is from C_{70} photoresponse. This can be understood as C_{70} loading in the blend films increases, more light can be absorbed by C_{70} in near UV and visible range, reaching 67% and 62%, respectively. Yet the efficiency shows strong light intensity dependence as can be seen in **Figure 4**d, indicating considerable non-germinated recombination most likely due to unbalanced and low charge mobilities.[7,30,31]

DIB-SQ loading in DIB-SQ:C_{70} film was further decreased to 1:5. The efficiency increased to 6.3% for the champion device with average efficiency over 6.0%. An EQE over 70% was observed from absorption of C_{70}, J_{sc} reaches 13.7 mA/cm^2, together with V_{oc} = 0.87 V and FF = 53%. As suggested by a previous study,[17] moderate carrier mobilities are sufficient to reach high efficiency of photovoltaic cells. Again, the light dependence of photovoltaic performance is still significant as shown in Figure 4. The PCE at low light intensity increases to ~8.0% corresponding to suppressed non-germinated recombination, which is a strong indication of the huge potential of organic photovoltaic cells —recombination losses can be effectively suppressed by improving film morphology and thus charge transport.

Considering the optical interference in thin film device, the optical field reaches its maxima 50 nm away from the reflective electrode. For our device architecture, generation of the excitons and charge carriers is more pronounced at the position close to ITO anode.[29] Therefore the average travel distance for holes to reach the anode is less than that of electrons to reach the cathode. C_{70} has relatively high electron mobility, ensuring efficient electron extraction by Al cathode. Further decreasing the DIB-SQ:C_{70} ratio results in enhanced FF and V_{oc}, however, decrease in photocurrent. The PCE remains above 5.5%, even when DIB-SQ:C_{70} ratio is 1:20. Our result is consistent with recent report by Tang's group, indicating the complicated mechanism of ambipolar charge transport in donor/acceptor blend films even with low donor concentration.[32] Increasing V_{oc} with lowering DIB-SQ to C_{70} ratio can be clearly observed, which should be directly related to the effects of Schottky junction between ITO/MoO_3 anode and C_{70}.[33]

Mobility is one of the key parameters that dominate charge carrier extraction. We measured carrier mobility based on space charge limited current (SCLC) model.[30] To have single carrier devices, 5-nm-thick MoO_3 is used as buffer layers on both side of blend films in hole-only devices, and 1-nm ultra-thin Ca[34] and BCP in electron-only devices. The calculated mobility values from three typical DIB-SQ:C_{70} blend ratio of 1:1, 1:5 and 1:10 are summarized in **Table 3**. The neat films of DIB-SQ and C70 have hole and electron mobility of 4.23×10^{-4} and 4.16×10^{-3} cm^2/Vs, respectively. Upon blending with 1:1 ratio, both electron and hole mobility are on the order of 10^{-4}, however, photocurrent is strongly field dependent. This could be due to the fact that high mobility may induce serious bimolecular recombination.[30] In 1:5 ratio device electron mobility increases by six times, and hole mobility slightly decreases. It indicates

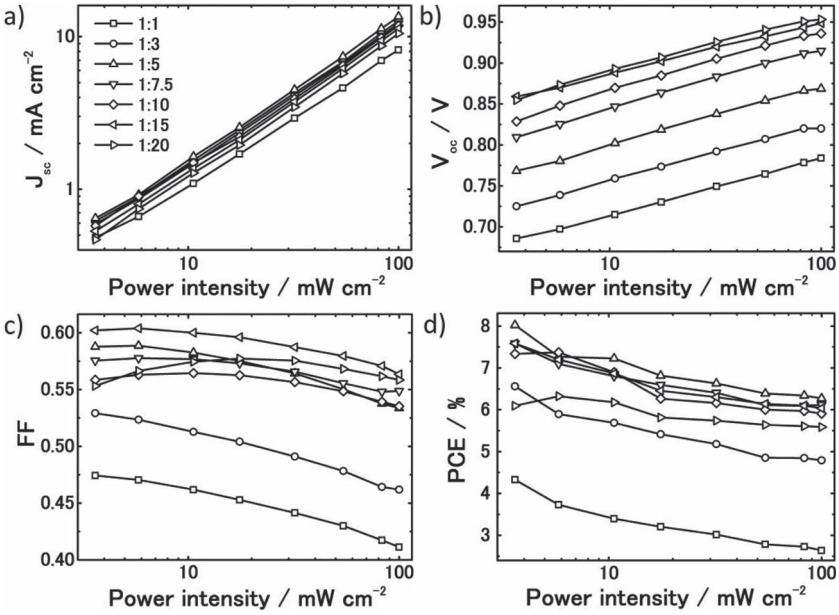

Figure 4. a) The short circuit current (J_{sc}), b) open circuit voltage (V_{oc}), c) fill factor (FF) and d) power conversion efficiency (PCE) versus power intensity for the device with different blend ratio.

Table 2. Summary of the key parameters in the DIB-SQ:C_{70} (1:5) cells with various layer thickness.

Thickness (nm)	J_{sc} [mA/cm^2]	V_{oc} [V]	FF	PCE (%) [P_0 = 1 sun]
30	7.0 ± 0.1	0.84 ± 0.01	0.61 ± 0.01	3.6 ± 0.1
50	11.8 ± 0.1	0.84 ± 0.01	0.55 ± 0.01	5.4 ± 0.2
60	13.6 ± 0.1	0.86 ± 0.01	0.52 ± 0.01	6.1 ± 0.2
70	14.3 ± 0.1	0.85 ± 0.01	0.47 ± 0.01	5.8 ± 0.2
80	14.5 ± 0.1	0.84 ± 0.01	0.45 ± 0.01	5.4 ± 0.2
90	14.3 ± 0.1	0.83 ± 0.01	0.44 ± 0.01	5.2 ± 0.2
110	13.0 ± 0.1	0.83 ± 0.01	0.40 ± 0.01	4.3 ± 0.2

Table 3. Carrier mobility data derived from single carrier devices using space charge limited current model.

Blend ratio	DIB-SQ	1:1	1:5	1:10	C_{70}
μ_h [cm^2/Vs]	4.23×10^{-4}	1.24×10^{-4}	9.81×10^{-5}	2.79×10^{-5}	–
μ_e [cm^2/Vs]	–	1.18×10^{-4}	6.75×10^{-4}	1.34×10^{-3}	4.16×10^{-3}

that electrons should be able to escape the blend films easily without meeting with their counterparts. The device shows large shunt resistance and small serial resistance. In 1:10 ratio device, the carrier mobilities are even more off balanced, resulting in efficient charge extraction, though PCE is limited by near infrared absorption.

Dependence of photovoltaic performance on light intensity proves that non-germinated recombination mainly limits the efficiency, even in the optimal ratio of 1:5. Figure 4 shows the photovoltaic parameters under varied incident power density. It is clear that when the incident power density decreases, FF and J_{sc} are improved, which are responsible for PCE enhancement. V_{oc} has a linear relationship with light intensity in logarithmic scale, subjective to classical semiconductor theory.[35]

To gain insight into the correlation between charge transport and film structure, atomic force microscope and x-ray diffraction are used to characterize film morphology. XRD shown in Supporting Information confirms that there are no patterns from any kind of aggregation from organic films. The peaks are from polycrystalline ITO film.

To further explore the charge transport properties in DIB-SQ:C_{70} blend films, we chose 1:5 ratio with varied thicknesses as shown in **Figure 5**, taking into account of the trade-off between charge transport and optical absorption. Independent from the film component, the film thickness becomes a critical parameter that determines charge extraction. In 1:5 DIB-SQ:C_{70} blend films, the film thickness is changed in a range from 30 nm to 110 nm. The key photovoltaic parameters are summarized in **Table 2**.

Starting from 30 nm cells, it is a minimum value that we can ensure uniform film of good quality. While V_{oc} of 0.85 V is normal values among all the devices, 62% FF is a high value for thermal deposited bulk heterojunctions without any additional treatments. It means that charge transport and collection in the device is quite efficient, resulting minor charge recombination loss. Limited mainly by the small thickness and insufficient light capturing, J_{sc} is only 7.05 mA/cm^2, and PCE of 3.7%.

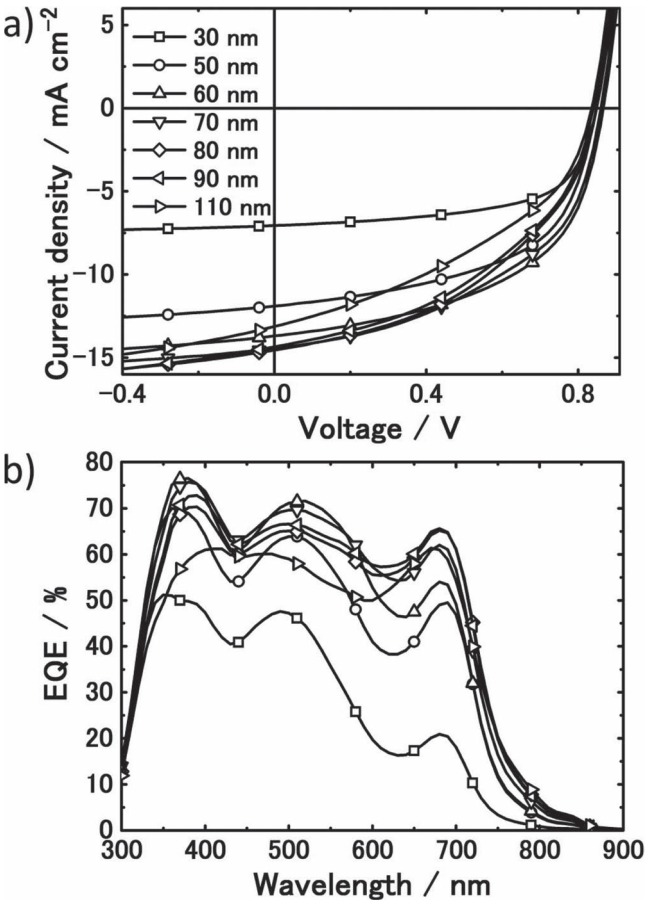

Figure 5. a) J–V characteristics illuminated under 100 mW/cm^2 AM 1.5G solar simulated light); b) EQE curves, of the 1:5 DIB-SQ:C_{70} photovoltaic cells with varied thickness.

Tuning the film thicknesses from 50 nm up to 80 nm, J_{sc} monotonously increases from 11.9 mA/cm^2 to 14.6 mA/cm^2. We noted that photovoltaic cells with thicknesses of 90 nm and 110 nm demonstrated decrease in J_{sc}. There are two possible reasons responsible for that. One is optical interference,[29] and the other could be that the charge extraction becomes less efficient, meaning charge recombination starts to compete strongly with extraction. Meanwhile it can be seen in Figure 5a that bright-state J–V curve of 110 nm thick device the largest slope at 0 V among the devices of varied thicknesses, and its FF is the lowest, consistent with the second reason.

From data summarized in **Figure 6**, Figure S2, Table 1 and 2, it shows that there is a relative large range for both thickness from 50 nm to 90 nm, and blending ratio from 1:5 to 1:20, in order to have PCE >5.5%. Such a property gives much tolerance for our device fabrication to reach optimal efficiency. Therefore it is important, especially for future industrial production which prefers to choose the system not sensitive to processing parameters.

In conclusion, we demonstrate high efficiency DIB-SQ:C_{70} based photovoltaic cells, reaching efficiency well above 6.0%. The effects of blending ratio and film thickness are discussed with respect to photovoltaic performance and optoelectronic

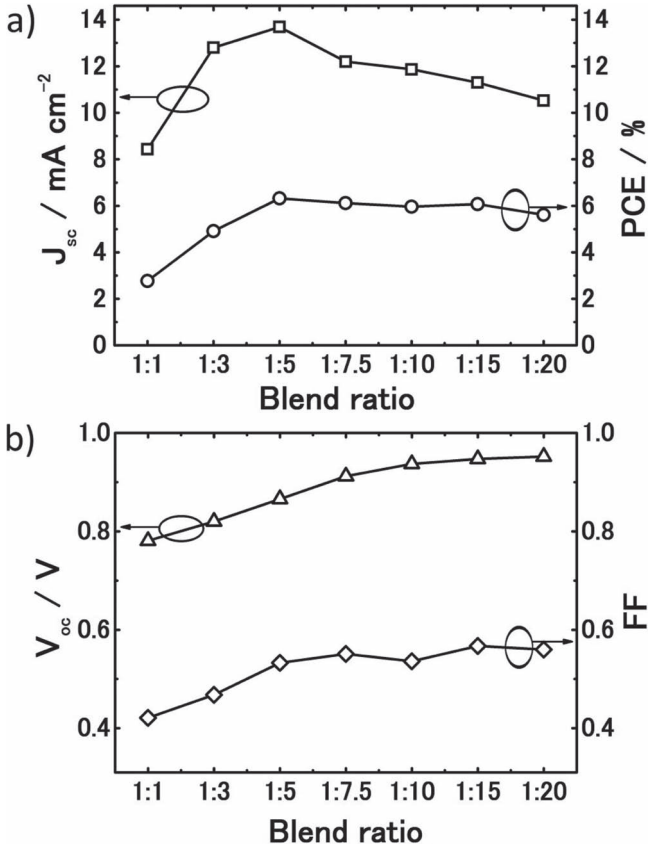

Figure 6. Photovoltaic characteristics of 60 nm-thick DIB-SQ:C_{70} cells with various blend ratios under AM 1.5G solar spectrum at 100 mW/cm^2 illumination. a) J_{sc} and PCE, b) V_{oc} and FF versus blend ratio.

properties in the donor:acceptor blend films. Our findings shows that PCE is, at least to some extent, not sensitive to blending ratio and film thickness, indicating DIB-SQ and its analogs are promising materials for future application in organic photovoltaics.

Experimental Section

DIB-SQ was synthesized according to the literature,[36] and further purified by using high vacuum sublimation system (with purity >99.9%). Commercially available C_{70} was sublimated >3 times before use. The patterned ITO substrates were cleaned sequentially using detergent, de-ionized water, acetone and isopropanol and exposed to ultraviolet ozone for 30 min. Then the substrates were transferred to a vacuum chamber with base pressure of 5×10^{-6} Pa. 4 nm MoO_3 was deposited on the ITO surface, then DIB-SQ and C_{70} were co-deposited. Finally the devices were completed by depositing the top electrode BCP (10 nm)/Al (100 nm) through a mask, leading to four solar cells on each substrate with an active area of 4.0 mm^2. For the devices with different donor:acceptor blend ratio or different active layer thickness, we fabricated 3 batches devices (16 cells per batch) in each of the case to obtain the average device performance. Single carrier devices were also fabricated with device structures of ITO/MoO_3 (4 nm)/DIB-SQ:C_{70} (1:x, 60 nm)/MoO_3 (4 nm)/Al (100 nm) and ITO/Ca (1 nm)/DIB-SQ:C_{70} (1:x, 60 nm)/BCP (10 nm)/Al (100 nm), with x represents loading of fullerene C_{70}, for electron and hole mobility, respectively. Both PCE and EQE characterizations of photovoltaic cells were carried out on a CEP-2000 integrated system by Bunkoukeiki Co. under standard measurement condition.[37] UV-visible absorption spectra were obtained using a SHIMADZU MPC-2200 UV-visible spectrophotometer.

Supporting Information

Supporting Information is available from the Wiley Online Library or from the author.

Acknowledgements

We thank financial support from the Japan Science and Technology Agency (JST) via the Japan Regional Innovation Strategy Program by the Excellence (J-RISE), and Adaptable and Seamless Technology transfer Program (A-STEP, AS232Z00929D). We thank Dr. K. Nakayama, Dr. D. Yokoyama, and Dr. J. Hu for technical assistance and scientific discussion. ZH thanks Dr C. J. Liang for stimulating discussion. We would also like to thank Mr. Steve Hawks for editorial assistance.

Received: January 17, 2012
Revised: February 10, 2012
Published online: April 18, 2012

[1] A. J. Heeger, *Chem. Soc. Rev.* **2010**, *39*, 2354.
[2] V. Coropceanu, J. Cornil, D. A. da Silva Filho, Y. Olivier, R. Silbey, J. L. Brédas, *Chem. Rev.* **2007**, *107*, 926.
[3] Y. Yang, F. Wudl, *Adv. Mater.* **2009**, *21*, 1401.
[4] Heliatek GmbH, press release,http://www.heliatek.com/?p=1346&lang=en.
[5] L. T. Dou, J. B. You, J. Yang, C. C. Chen, Y. J. He, S. Murase, T. Moriarty, K. Emery, G. Li, Y. Yang, *Nat. Photonics* **2012**, *6*, 180.
[6] H. Ohkita, S. Cook, Y. Astuti, W. Duffy, S. Tierney, W. Zhang, M. Heeney, I. McCulloch, J. Nelson, D. D. C. Bradley, J. R. Durrant, *J. Am. Chem. Soc.* **2008**, *130*, 3030.
[7] C. Deibel, *Phys. Status. Solidi A-Appl. Mater. Sci.* **2009**, *206*, 2731.
[8] L. M. Chen, Z. Xu, Z. R. Hong, Y. Yang, *J. Mater. Chem.* **2010**, *20*, 2575.
[9] J. K. Lee, W. L. Ma, C. J. Brabec, J. Yuen, J. S. Moon, J. Y. Kim, K. Lee, G. C. Bazan, A. J. Heeger, *J. Am. Chem. Soc.* **2008**, *130*, 3619.
[10] G. D. Wei, S. Y. Wang, K. Sun, M. E. Thompson, S. R. Forrest, *Adv. Energy Mater.* **2011**, *1*, 184.
[11] G. Li, V. Shrotriya, J. Huang, Y. Yao, T. Moriarty, K. Emery, Y. Yang, *Nat. Mater.* **2005**, *4*, 864.
[12] a) N. M. Kronenberg, V. Steinmann, H. Bürckstümmer, J. Hwang, D. Hertel, F. Würthner, K. Meerholz, *Adv. Mater.* **2010**, *22*, 4193; b) X. D. Dang, A. B. Tamayo, J. Seo, C. V. Hoven, B. Walker, T. Q. Nguyen, *Adv. Func. Mater.* **2010**, *20*, 3314.
[13] K. Schulze, C. Uhrich, R. Schüppel, K. Leo, M. Pfeiffer, E. Brier, E. Reinold, P. Bäuerle, *Adv. Mater.* **2006**, *18*, 2872.
[14] Y. Liu, X. Wan, F. Wang, J. Zhou, G. Long, J. Tian, J. You, Y. Yang, Y. Chen, *Adv. Energy Mater.* **2011**, *1*, 771.
[15] S. R. Forrest, *Chem. Rev.* **1997**, *97*, 1793.
[16] H. Sasabe, J. Kido, *Chem. Mater.* **2011**, *23*, 621.
[17] K. Walzer, B. Maennig, M. Pfeiffer, K. Leo, *Chem. Rev.* **2007**, *107*, 1233.
[18] B. Maennig, J. Drechsel, D. Gebeyehu, P. Simon, F. Kozlowski, A. Werner, F. Li, S. Grundmann, S. Sonntag, M. Koch, K. Leo, M. Pfeiffer, H. Hoppe, D. Meissner, N. S. Sariciftci, I. Riedel, V. Dyakonov, J. Parisi, *Appl. Phys. A: Mater. Sci. Proc.* **2004**, *79*, 1.
[19] P. Peumans, S. R. Forrest, *Appl. Phys. Lett.* **2001**, *79*, 126.

[20] F. Silvestri, M. D. Irwin, L. Beverina, A. Facchetti, G. A. Pagani, T. J. Marks, *J. Am. Chem. Soc.* **2008**, *130*, 17640.
[21] F. Silvestri, I. López-Duarte, W. Seitz, L. Beverina, M. V. Martínez-Díaz, T. J. Marks, D. M. Guldi, G. A. Pagani, T. Torres, *Chem. Commun.* **2009**, 4500.
[22] D. Bagnis, L. Beverina, H. Huang, F. Silvestri, Y. Yao, H. Yan, G. A. Pagani, T. J. Marks, A. Facchetti, *J. Am. Chem. Soc.* **2010**, *132*, 4074.
[23] U. Mayerhöffer, K. Deing, K. Gruβ, H. Braunschweig, K. Meerholz, F. Würthner, *Angew. Chem. Int. Ed.* **2009**, *48*, 8776.
[24] S. Y. Wang, E. I. Mayo, M. D. Perez, L. Griffe, G. D. Wei, P. I. Djurovich, S. R. Forrest, M. E. Thompson, *Appl. Phys. Lett.* **2009**, *94*, 233304.
[25] Y. Zhao, Z. Y. Xie, Y. Qu, Y. H. Geng, L. X. Wang, *Appl. Phys. Lett.* **2007**, *90*, 043504.
[26] V. Steinmann, N. M. Kronenberg, M. R. Lenze, S. M. Graf, D. Hertel, K. Meerholz, H. Bürckstümmer, E. V. Tulyakova, F. Würthner, *Adv. Energy Mater.* **2011**, *1*, 888.
[27] V. Shrotriya, G. Li, Y. Yao, C. Chu, Y. Yang, *Appl. Phys. Lett.* **2006**, *88*, 073508.
[28] J. Meyer, R. Khalandovsky, P. Görrn, A. Kahn, *Adv. Mater.* **2011**, *23*, 70.
[29] P. Peumans, A. Yakimov, S. R. Forrest, *J. Appl. Phys.* **2003**, *93*, 3693.
[30] P. W. M. Blom, V. D. Mihailetchi, L. J. A. Koster, D. E. Markov, *Adv. Mater.* **2007**, *19*, 1551.
[31] J. Yang, R. Zhu, Z. R. Hong, Y. He, A. Kumar, Y. F. Li, Y. Yang, *Adv. Mater.* **2011**, *23*, 3465.
[32] M. L. Zhang, H. Wang, H. K. Tian, Y. H. Geng, C. W. Tang, *Adv. Mater.* **2011**, *23*, 4960.
[33] M. L. Zhang, Irfan, H. J. Ding, Y. L. Gao, C. W. Tang, *Appl. Phys. Lett.* **2010**, *96*, 183301.
[34] C. Y. Jiang, X. W. Sun, D. W. Zhao, A. K. K. Kyaw, Y. N. Li, *Sol. Energy Mater. Sol. Cells* **2010**, *94*, 1618.
[35] J. Nelson, *The Physics of Solar Cells*, ISBN 1-86094-340-3, Imperial College Press: London, U.K., **2003**.
[36] M. Q. Tian, M. Furuki, I. Iwasa, Y. Sato, L. S. Pu, S. Tatsuura, *J. Phys. Chem. B* **2002**, *106*, 4370.
[37] V. Shrotriya, G. Li, Y. Yao, T. Moriarty, K. Emery, Y. Yang, *Adv. Funct. Mater.* **2006**, *16*, 2016.